Application of Cagniard de Hoop Method to the Analysis of Perfectly Matched Layers

Julien Diaz * **Patrick Joly** **

* *EPI Magique 3D, INRIA Bordeaux Sud-Ouest, Bâtiment IPRA - Université de Pau et des Pays de l'Adour Avenue de l'Université - BP 1155 - F64013 Pau cedex e-mail: julien.diaz@inria.fr).*
** *Poems UMR 27 06, INRIA Paris Rocquencourt, Domaine de Voluceau – BP 105- F78153 Le Chesnay (e-mail: patrick.joly@inria.fr)*

Abstract: We show how Cagniard de Hoop method can be used, first to obtain error estimates for the Perfectly Matched Layers in acoustics (PML), then to understand the instabilities of the PML when applied to aeroacousics. The principle of the methods consists in applying to the equations a Laplace transform in time and a Fourier transform in one space variable to obtain an ordinary differential equation which can be explicitely solved. This solution contains a pseudo-differential term $1/\left(s^2/c^2+k_x^2\right)^{\frac{1}{2}}$ and the key point of the method is to find path in the complex plan to turn this term into the well-known solution of the 2D wave equation $1/\sqrt{t^2-r^2/c^2}$. We illustrate our results through comparison with numerical computation.

Keywords: Boundary Conditions, Error Analysis, Stability Analysis, Time-domain Analysis, Wave equation, Laplace Transforms, Fourier Transforms

1. INTRODUCTION

The Perfectly Matched Layer (PML) method has been introduced by Bérenger (1996) to simulate the propagation of transient waves in infinite media. Its principle consists on surrounding the computational domain, which is necessarily bounded, by an absorbing layer which has the astonishing property not to generate any reflection at its interface with the computational domain. This is achieved by adding to the wave equation a very special damping term, acting only in the direction orthogonal to the layer.

When one uses such a technique in a computational code, it is important to prove the stability property of the new equations and to evaluate the reflection produced by the end of the PML layer. Cagniard de Hoop method (Cagniard (1939, 1962); de Hoop (1959)), introduced by Cagniard in 1930 to obtain analytical solution of the elastodynamics equation, appears to be a very useful tool to address this two questions. Indeed, it allows us to analytically compute the Green function of transient waves propagation problem in stratified media, such as the PML. Then, using a time convolution between the source function and the Green function, we compute the expression of the waves reflected by the PML.

The second step of the method consists in applying an inverse Fourier in the x variable to this solution and, by choosing an appropriate contour in the complex plane, to turn this inverse Fourier transform into a Laplace transform where the integrand is nothing but the analytical solution of the reflected wave.

The first part of the paper concern the acoustics wave equation in two dimension. We show how the use of the Cagniard-de Hoop technique can provide the Green function of the half-space problem bounded by a finite PML and how we can derive error estimates from this analytical solution. In A. T. de Hoop and Remis (2001), de Hoop, van der Berg and Remis applied this technique to obtain the analytic solution of the wave reflected by the PML, but without deriving error estimates from it. The results we present here are presented with more details in Diaz and Joly (2006).

In the second part we will focus on the aeroacoustic waves equation. In this case, the classical PML technique is unstable and the instabilities can be analyzed thanks to a plane wave analysis (see Bécache et al. (2003)). This analysis is however restricted to the high-frequency waves. We present here another way to analyse the instabilities in the time-domain, whatever the frequency of the waves, thanks to the Cagniard-de Hoop method. This analysis can be regarded as a complement of the plane waves analysis and gives a better understanding of the behaviour of the unstable waves in the PML.

The results we present here are presented with more details in Diaz and Joly (2006). The Cagniard-de Hoop can also be applied to obtain error estimates for absorbing boundary conditions A. T. de Hoop and Remis (2001); Diaz and Joly (2005).

2. THE PML FOR ACOUSTICS

2.1 The equations of the PML

In this section we focus on the solution of the wave equation in the whole plane $\mathbb{R}^2$ with a point source in space located in $(0,h)$:

$$\frac{1}{c^2}\frac{\partial^2 u_i}{\partial t^2} - \frac{\partial^2 u_i}{\partial x^2} - \frac{\partial^2 u_i}{\partial y^2} = \delta_x \delta_{y-h} f(t) \quad \text{in } \mathbb{R}^2, \qquad (1)$$

where c is celerity of the waves. Let us know suppose that we only want to compute u in the upper half-space $y > 0$. This can be achieved by adding a horizontal layer of width L in which eq. (1) is modified by an absorption term (see Fig. 1).

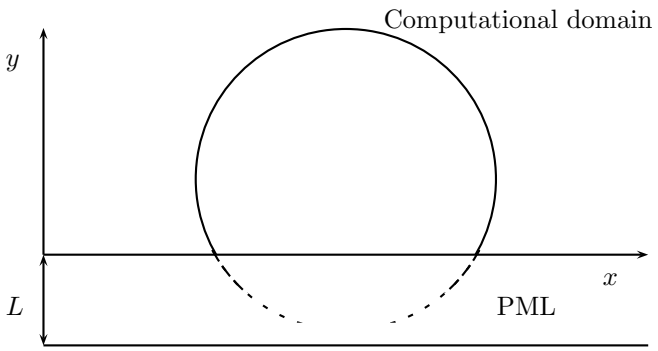

Fig. 1. Computational Domain and PML.

In Bérenger (1996) Bérenger proposed a very special absorption term, acting only on the direction orthogonal to the layer, by replacing the operator of derivation with respect to y by the operator D_y^σ, formally defined by:

$$D_y^\sigma = \left(\frac{\partial}{\partial t} + \sigma(y)\right)^{-1} \frac{\partial}{\partial t}\frac{\partial}{\partial y}$$

more precisely, if $\psi = D_y^\sigma \phi$, then ψ is solution of

$$\left(\frac{\partial}{\partial t} + \sigma(y)\right)\psi = \frac{\partial}{\partial t}\frac{\partial}{\partial y}\phi \text{ and } \psi(t=0) = 0.$$

If we extend σ in the upper half plane by $\sigma(y) = 0$ for $y > 0$, the problems we have to solve can be rewritten as

$$\begin{cases} \dfrac{1}{c^2}\dfrac{\partial^2 u}{\partial t^2} - \dfrac{\partial^2 u}{\partial x^2} - (D_y^\sigma)^2 y = \delta_x \delta_{y-h} f(t) & \text{for } -L < y, \\ \dfrac{\partial u}{\partial y} = 0, & \text{for } y = -L \end{cases} \qquad (2)$$

As we said before, this layer does not produce any reflection at the interface $y = 0$, moreover the waves are *exponentially damped* in the layer. However, for numerical reasons, the width of the layer L should be finite and a Neumann condition is usually imposed at its end. The waves are then reflected at the end of the PML and come back to the domain. Even if the waves are strongly damped, it is important to estimate this reflections, especially when one wants to validate a numerical code.

2.2 Computation of the Green function of system (2)

Cagniard-de Hoop method seems to be the most appropriate tools to estimate the importance of the reflections produced by the PML layers. It allows us to compute the solution of the Green function of eq. (2), i.e. the solution of:

$$\begin{cases} \dfrac{1}{c^2}\dfrac{\partial^2 G}{\partial t^2} - \dfrac{\partial^2 G}{\partial x^2} - (D_y^\sigma)^2 G = \delta_x \delta_{y-h}\delta(t) & \text{for } -L < y, \\ \dfrac{\partial G}{\partial y} = 0 & \text{for } y = -L. \end{cases}$$

The idea of the method is to perform a Laplace transform in time and a Fourier transform in the space variable which is parallel to the interface between the two media (x in this case) to obtain an ordinary differential equation which can be explicitely solved. The second step of the method consists in applying an inverse Fourier in the x variable to this solution and, by choosing an appropriate contour in the complex plane, to turn this inverse Fourier transform into a Laplace transform where the integrand is nothing but the analytical solution of the reflected wave.

Before doing so, let us first remark that, since we impose a Neumann condition on the external boundary $y = -L$, we can deduce from the image principle that $G = G^i + G^r$ where G^i if the solution of

$$\frac{1}{c^2}\frac{\partial^2 G^i}{\partial t^2} - \frac{\partial^2 G^i}{\partial x^2} - (D_y^\sigma)^2 G^i = \delta_x \delta_{y-h}\delta(t), (x,y) \in \mathbb{R}^2 \qquad (3)$$

with $\sigma_y(y) = \sigma_y(-y - 2L)$ for $y < -L$ (i.e. we extend σ_y to the half-plane $y < -L$ by symmetry with respect to the axis $y = -L$) and $G^r(x, y, t) = G^i(x, -y - 2L, t)$ for $y \geq -L$ (see Fig. 2).

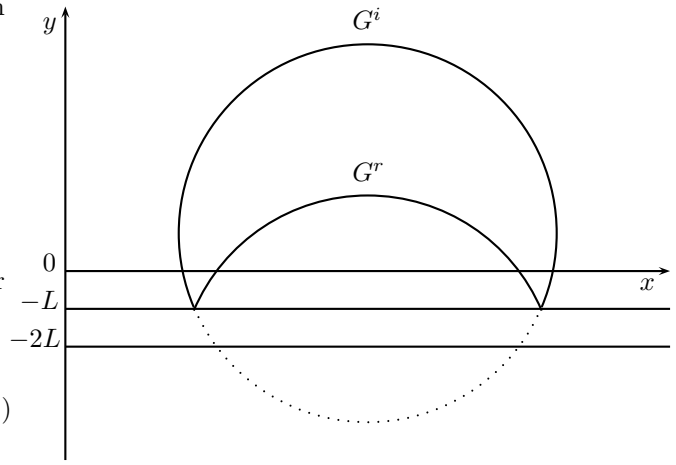

Fig. 2. Incident and reflected field.

Therefore we only have to compute G^i, which represents the incident wave, by Cagniard-de Hoop method to deduce the reflected wave G^r.

Let us now apply a Laplace transform in time and a Fourier transform in the x variable to eq. (3):

$$-\frac{s}{s+\sigma(y)}\frac{d}{dy}\left(\frac{s}{s+\sigma(y)}\frac{d\hat{G}^i}{dy}\right) + \left(\frac{s^2}{c^2} + k^2\right)\hat{G}^i = \delta_{y-h}, y \in \mathbb{R} (4)$$

After the change of variable

$$Y = y + \frac{1}{s}\Sigma(y), \text{ with } \Sigma(y) = \int_0^y \sigma(v)dv,$$

we obtain

$$-\frac{d^2\hat{\mathcal{G}}^i}{dy^2}+\left(\frac{s^2}{c^2}+k^2\right)\hat{\mathcal{G}}^i=\delta_{y-h},\quad y\in\mathbb{R}. \tag{5}$$

where

$$\hat{\mathcal{G}}^i(k,Y,s)=\hat{G}^i(k,y+\frac{1}{s}\Sigma(y),s)$$

It is well known that the solution of (5) is

$$\hat{\mathcal{G}}^i(k,Y,s)=\frac{e^{-\left(k^2+\frac{s^2}{c^2}\right)^{\frac{1}{2}}|Y-h|}}{2\left(k^2+\frac{s^2}{c^2}\right)^{\frac{1}{2}}},$$

or, back to the y variable:

$$\hat{G}^i(k,y,s)=\frac{e^{-\left(k^2+\frac{s^2}{c^2}\right)^{\frac{1}{2}}|y-h-\frac{1}{s}\Sigma(y)|}}{2\left(k^2+\frac{s^2}{c^2}\right)^{\frac{1}{2}}}.$$

Let us remark that, if $y>0$, $\Sigma(y)=0$ and

$$\hat{G}^i(k,y,s)=\frac{e^{-\left(k^2+\frac{s^2}{c^2}\right)^{\frac{1}{2}}|y-h|}}{2\left(k^2+\frac{s^2}{c^2}\right)^{\frac{1}{2}}},$$

which is the Fourier-Laplace transform of the fundamental solution of the 2D wave equation. Let us now suppose that $y<0$. Obviously

$$y-h-\frac{1}{s}\Sigma(y)<0$$

and

$$\hat{G}^i(k,y,s)=\frac{e^{\left(k^2+\frac{s^2}{c^2}\right)^{\frac{1}{2}}\left(y-h-\frac{1}{s}\Sigma(y)\right)}}{2\left(k^2+\frac{s^2}{c^2}\right)^{\frac{1}{2}}}.$$

Let us now apply an inverse Fourier transform to $\hat{G}^i(k,y,s)$ to obtain

$$\tilde{G}^i(x,y,s)=\int_{-\infty}^{+\infty}\frac{e^{\left(k^2+\frac{s^2}{c^2}\right)^{\frac{1}{2}}\left(y-h-\frac{1}{s}\Sigma(y)\right)-ikx}}{4\pi\left(k^2+\frac{s^2}{c^2}\right)^{\frac{1}{2}}}dk.$$

By denoting $k=ps/c$, we have

$$\begin{aligned}\tilde{G}^i(x,y,s)&=\int_{-\infty}^{+\infty}\frac{e^{-\frac{\Sigma(y)}{c}(1+p^2)^{\frac{1}{2}}}}{4\pi\left(1+p^2\right)^{\frac{1}{2}}}e^{-\frac{s}{c}\left(ipx-(1+p^2)^{\frac{1}{2}}(y-h)\right)}dp.\\&=\int_{-\infty}^{+\infty}\Psi(p)dp.\end{aligned}$$

Now, the key point of the method is to find a path in the complex plane so that the term in the exponential becomes

$$ipx-(1+p^2)^{\frac{1}{2}}(y-h)=ct\in\mathbb{R}^+, \tag{6}$$

so that we can turn the above Fourier transform into a one-sided Laplace transform:

$$\tilde{G}^i(x,y,s)=\int_0^{+\infty}F(t)e^{-st}dt.$$

Then we'll deduce that $\tilde{G}^i(x,y,.)$ is the Laplace transform of F and, using the injectivity of the Laplace transform that $G^i(x,y,t)=F(t)$.

Since we are using a path in the complex plane, it is necessary to define the square root function $(p)^{\frac{1}{2}}$ for $p\in\mathbb{C}$ and to determine the branch cuts of the function $(1+p^2)^{\frac{1}{2}}$.

Definition 1. For $p\in\mathbb{C}\backslash\mathbb{R}^-$, we use the following definition of the square root $g(p)=p^{\frac{1}{2}}$:

$$g(p)^2=p\quad\text{and}\quad\Re e[g(p)]>0.$$

The branch cut of $g(p)$ in the complex plane is thus the half-line defined by $\{p\in\mathbb{R}^-\}$ (see Fig. 3) and the branch cuts of $(1+p^2)^{\frac{1}{2}}$ are the two half lines defined by

$$\{\Re e(p)=0\text{ and }|p|>1\}$$

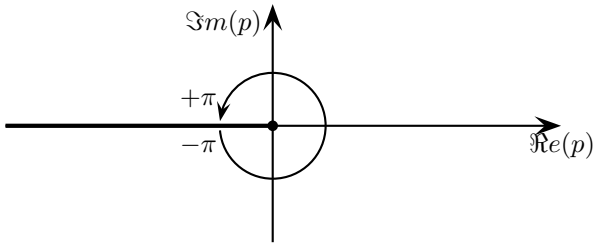

Fig. 3. Definition of the function $x\mapsto(x)^{\frac{1}{2}}$

To simplify the calculation, let us first define the polar coordinates (r,θ) of (x,y) with respect to the point source $(0,h)$:

$$x=r\cos\theta\text{ and }y-h=r\sin\theta.$$

Eq. (6) then becomes

$$ip\cos\theta-(1+p^2)^{\frac{1}{2}}\sin\theta=\frac{ct}{r},\ t\in\mathbb{R}^+. \tag{7}$$

Obviously, each solution p of (7) is a root of the second order polynomial

$$P(t)=p^2+2\mathrm{i}\frac{ct}{r}\cos\theta p+\sin^2\theta-\frac{c^2t^2}{r^2}$$

and we easily prove that, for $t>t_0=\frac{r}{c}$, the two roots $p=\gamma^{\pm}(t)$ of P defined by

$$\gamma^{\pm}(t)=-\mathrm{i}\frac{ct}{r}\cos\theta\mp\sin\theta\sqrt{\frac{c^2t^2}{r^2}-1}$$

are solution of (7) (let us recall that we consider $y<0$ so that $\sin\theta<0$). $\gamma^+(t_0)=\gamma^-(t_0)=-\mathrm{i}\cos\theta$ is imaginary and does not lie on the branch cuts of the function $(1+p^2)^{\frac{1}{2}}$. We now define the path Γ_R by

$$\begin{cases}\Gamma_R=\Gamma_R^+\cup\Gamma_R^-\\ \Gamma_R^{\pm}=\{p=\gamma^{\pm}(t),t_0\le t\le(1+R)t_0\},\end{cases}$$

We denote by D_R the real segment $[-|\gamma^-(R)|\,;|\gamma^+(R)|]$ and we close the path by the two arcs of circle C_R^+ and C_R^- which join Γ_R and D_R together (see fig 4).

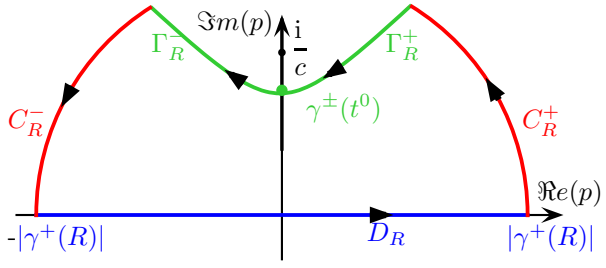

Fig. 4. Integration path.

By Cauchy's theorem :

$$\int_{D_R} \Psi(p)dp + \int_{C_R^+} \Psi(p)dp + \int_{\Gamma_R} \Psi(p)dp + \int_{C_R^-} \Psi(p)dp = 0.$$

Moreover, by using Jordan's lemma, we have:

$$\lim_{R\to\infty} \int_{C_R^\pm} \Psi(p)dp = 0,$$

then

$$\int_{-\infty}^{+\infty} \Psi(p)dp = -\int_{\Gamma_{+\infty}} \Psi(p)dp = -\int_{\Gamma_{+\infty}^+} \Psi(p)dp - \int_{\Gamma_{+\infty}^-} \Psi(p)dp.$$

Let us now use the change of variable $p = \gamma^\pm(t)$ on $\Gamma_{+\infty}^\pm$:

$$\begin{aligned}\tilde{G}^i(x,y,s) = &-\int_{t_0}^{+\infty} \frac{e^{-\frac{\Sigma(y)}{c}(1+\gamma^{-2}(t))^{\frac{1}{2}}}}{4\pi\left(1+\gamma^{-2}(t)\right)^{\frac{1}{2}}} \frac{d\gamma^-(t)}{dt} e^{-st}dt \\ &+ \int_{t_0}^{+\infty} \frac{e^{-\frac{\Sigma(y)}{c}(1+\gamma^{+2}(t))^{\frac{1}{2}}}}{4\pi\left(1+\gamma^{+2}(t)\right)^{\frac{1}{2}}} \frac{d\gamma^+(t)}{dt} e^{-st}dt.\end{aligned}$$

After some calculations, we obtain:

- $\dfrac{1}{\left(1+\gamma^{\pm 2}(t)\right)^{\frac{1}{2}}} \dfrac{d\gamma^\pm(t)}{dt} = \pm \dfrac{dt}{\sqrt{t^2 - \frac{r^2}{c^2}}}$
- $\left(1+\gamma^{\pm 2}(t)\right)^{\frac{1}{2}} = -\dfrac{t}{r}\sin\theta \mp \mathrm{i}\dfrac{\cos\theta}{r}\sqrt{t^2-\dfrac{r^2}{c^2}}.$

so that

$$\begin{aligned}\tilde{G}^i(x,y,s) = &\int_{t_0}^{+\infty} \frac{e^{\left(\frac{t}{r} - \mathrm{i}\frac{\cos\theta}{r}\sqrt{t^2-\frac{r^2}{c^2}}\right)\sin\theta\Sigma(y)}}{4\pi\sqrt{t^2-\frac{r^2}{c^2}}} e^{-st}dt \\ &+ \int_{t_0}^{+\infty} \frac{e^{\left(\frac{t}{r} + \mathrm{i}\frac{\cos\theta}{r}\sqrt{t^2-\frac{r^2}{c^2}}\right)\sin\theta\Sigma(y)}}{4\pi\sqrt{t^2-\frac{r^2}{c^2}}} e^{-st}dt.\end{aligned}$$

Finally

$$\tilde{G}^i(x,y,s) = \int_{t_0}^{+\infty} \frac{e^{\frac{t}{r}\sin\theta\Sigma(y)}}{2\pi\sqrt{t^2-\frac{r^2}{c^2}}} \cos\left[\frac{\cos\theta}{r}\sqrt{t^2-\frac{r^2}{c^2}}\right] e^{-st}dt.$$

Using the injectivity of the one-sided Laplace transform we deduce that

$$G^i(x,y,t) = \frac{H(t-\frac{r}{c})}{2\pi\sqrt{t^2-\frac{r^2}{c^2}}} e^{\frac{t}{r}\sin\theta\Sigma(y)} \cos\left[\frac{\cos\theta}{r}\sqrt{t^2-\frac{r^2}{c^2}}\right].$$

where H denotes the Heavyside step function function. The reflected Green function is then computed thanks to the image principle:

$$\begin{aligned}&G^r(x,y,t) = G^i(x,-y-2L,t) \\ &= \frac{H(t-\frac{r^\star}{c})}{2\pi\sqrt{t^2-\frac{r^{\star 2}}{c^2}}} e^{-\frac{t}{r^\star}\sin\theta^\star\Sigma(y)} \cos\left[\frac{\cos\theta^\star}{r^\star}\sqrt{t^2-\frac{r^{\star 2}}{c^2}}\right],\end{aligned}$$

where $r^\star$ and $\theta^\star$ are defined by:

$$x = r^\star\cos\theta^\star \text{ and } y+h+2L = r^\star\sin\theta^\star,$$

and are actually the polar coordinates of (x,y) with respect to the image point source $(0,-h-2L)$ (see Fig. 5)

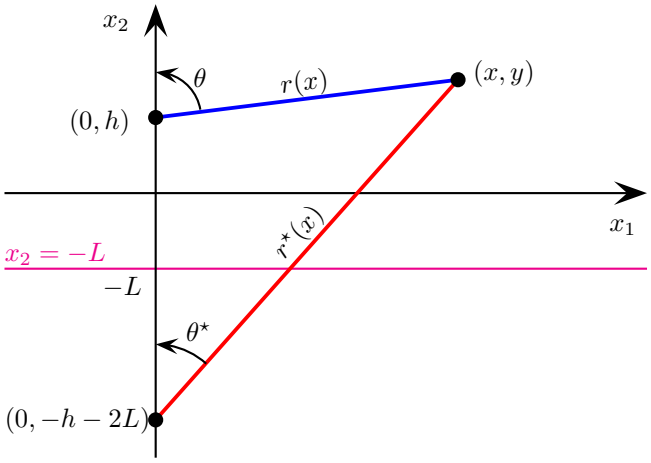

Fig. 5. Illustration of the notations

2.3 Error estimates

We are now able to compute the error $e = u_i - u$, where u_i is solution of (1) and u is solution of (2). This error is actually the wave reflected by the end of the PML:

$$e(x,y,t) = G^r(x,y,.) * f = \int_{t_0}^{t} G^r(x,y,\tau) f(t-\tau)d\tau$$

If the source function is such that $f(t) = 0$ for $t > T$, then

$$\begin{cases} |e(x,y,t)| \le \|f\|_{L^\infty(0,t)} \cdot \|G(x,y,.)\|_{L^1(t_0,t)} & \text{if } t_0 \le t \le t_0+T, \\ |e(x,y,t)| \le \|f\|_{L^\infty(0,T)} \cdot \|G(x,y,.)\|_{L^1(t-T,t)} & \text{if } t > t_0+T. \end{cases}$$

To obtain an uniform estimate of the error we thus have to compute $\max_{x,y} \|G(x,y,.)\|_{L^1(t_0,t)}$ if $t_0 \le t \le t_0+T$ and $\max_{x,y} \|G(x,y,.)\|_{L^1(t-T,t)}$ if $t > t_0+T$ (see Diaz and Joly (2006) for the details of the computation):

$$\begin{cases} \max_{x,y} \|G(x,y,.)\|_{L^1(t_0,t)} \le \\ \dfrac{e^{-\frac{2(2L+h)\Sigma(L)}{c^2 t}}}{2\pi} \mathrm{Log}\left(\dfrac{ct}{r^\star} + \sqrt{\dfrac{c^2t^2}{r^{\star\frac{1}{2}}} - 1}\right) \text{ if } t_0 \le t \le t_0+T \\ \max_{x,y} \|G(x,y,.)\|_{L^1(t-T,t)} \le \\ \dfrac{e^{-\frac{2(2L+h)\Sigma(L)}{c^2(t-T)}}}{2\pi} \mathrm{Log}\left(\dfrac{t+\sqrt{t^2-(t-T)^2}}{t-T}\right) \text{ if } > t_0+T. \end{cases}$$

2.4 Numerical results

To illustrate our results, with have compared our analytical solution with the one obtained by a numerical code. The source is located at a distance $h = 0.5$ from the PML and the time source is a truncated first derivative of a gaussian:

$$f(t) = \frac{d}{dt}\left\{e^{-2\pi f_0(t-t0)^2}\right\} H(2t0-t),\ f0 = 10,\ t0 = 1/f0.$$

The width of the PML is 0.1 and the damping function σ is such that:

$$\sigma(y) = \sigma_0 y^2, \text{ with } \sigma_0 = 50.10^3.$$

The total fields computed by the analytical solution (top picture) and by the numerical code (bottom picture) are represented in Fig. 6 and the reflected fields are

represented in Fig. 7 at time $t = 0.4$. In Fig. ?? and ?? we represent respectively the total and reflected field at point $(0.9, 0.1)$ with respect to the time. The blue curves represent the analytical solution and the red curves the numerical one.

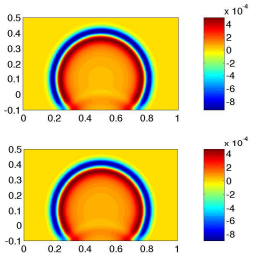

Fig. 6. Total Field at $t = 0.4$.

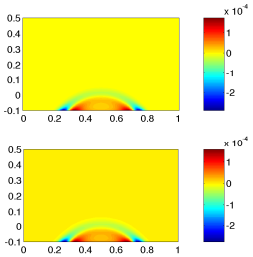

Fig. 7. Reflected Field at $t = 0.4$.

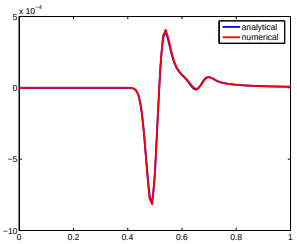

Fig. 8. Total Field at $(x, y) = (0.9, 0.1)$.

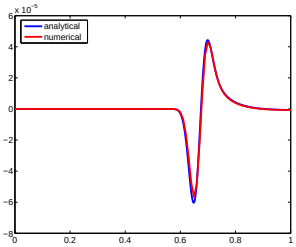

Fig. 9. Reflected Field at $(x, y) = (0.9, 0.1)$.

3. THE PML FOR AEROACOUSTICS

3.1 The equations of the PML

In this section we consider the second order formulation of the equation of subsonic aeroacoustics with a mean flow parallel to the x axis:

$$\frac{1}{c^2}\frac{\partial^2 u}{\partial t^2} + 2M\frac{\partial^2 u}{\partial x \partial t} - (1-M^2)\frac{\partial^2 u}{\partial x^2} - \frac{\partial^2 u}{\partial y^2} = \delta_{x+h}\delta_y f(t) \quad (8)$$

where M is the Mach number, $|M| < 1$ and $h > 0$.

As for the acoustics case, the classical model of a vertical PML for aeroacoustics is obtained by replacing the operator of derivation with respect to x par the operator D_x^σ:

$$\frac{\partial^2 u}{\partial t^2} + 2M\frac{\partial}{\partial t}D_x^\sigma u - (1-M^2)(D_x^\sigma)^2 u - \frac{\partial^2 u}{\partial y^2} = \delta_{x+h}\delta_y f(t) \quad (9)$$

It is now well-known that the classical PML for this equation are unstable : some waves increase exponentially in the vertical layers instead of being damped. These instabilities have been studied in Bécache et al. (2003): this analysis shows that the instabilities are due to the presence of so-called back-propagative waves, whose group and phase velocity vectors have opposite directions. However this work was restricted to the case of high frequency, which is sufficient to prove instability, but can not be applied to prove the stability of other type of PML (it does not prove the stability of low-frequency waves). Thanks to Cagniard-de Hoop method, we have proved the instability of the PML, whatever the frequency of the wave, and we have been able to prove the stability of modified PML for aeroacoustics.

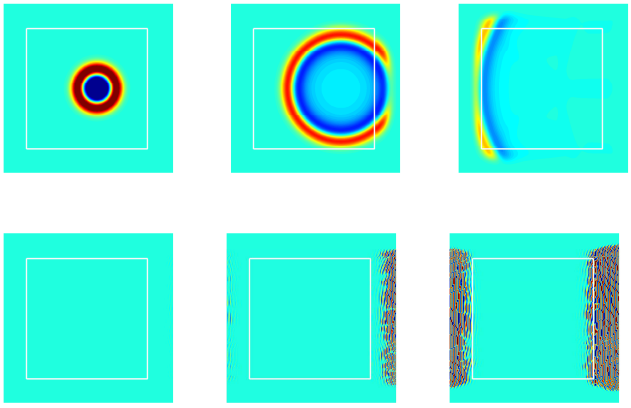

Fig. 10. The instabilities in the horizontal PML.

As we are only interested in the stability of the layer and not in the estimation of the error, we will consider here the case of an infinite layer and solve (9) on $\mathbb{R}^2$. Therefore, we define $\sigma(x) = 0$ for $x \leq 0$ and $\sigma(x) > 0$ for $x > 0$.

3.2 Computation of the Green Function

Once again, we first have to solve the Green problem

$$\frac{\partial^2 G}{\partial t^2} + 2M\frac{\partial}{\partial t}D_x^\sigma G - (1-M^2)(D_x^\sigma)^2 G - \frac{\partial^2 G}{\partial y^2} = \delta_{x+h}\delta_y\delta_t \quad (10)$$

and then to convolve G with the source function f to compute u. After having applied a Laplace transform and a Fourier transform in the y variable we obtain:

$$-(1-M^2)(\hat{D}_x^\sigma)^2\hat{G} + 2Ms\hat{D}_x^\sigma\hat{G} + \left(\frac{s^2}{c^2} + k^2\right)\hat{G} = \delta_{x+h}, \quad (11)$$

where

$$\hat{D}_x^\sigma = \frac{s}{s+\sigma(x)}\frac{d}{dx}.$$

The solution of (11) is

$$\hat{G}(x,k,s) = \frac{e^{\frac{s(x+h)+\Sigma(x)}{1-M^2}\left(M-\sqrt{1+(1-M^2)\frac{k^2}{s^2}}\right)}}{2\sqrt{s^2+(1-M^2)k^2}},$$

with

$$\Sigma(x) = \int_0^x \sigma(v)dv.$$

Let us now apply an inverse Fourier transform to y to obtain (after having set $k = \frac{ps}{\sqrt{1-M^2}}$):

$$\tilde{G}(x,y,s) = \int_{-\infty}^{+\infty} \frac{e^{\Sigma(x)\frac{M-\sqrt{1+p^2}}{1-M^2}} e^{s\left[(x+h)\frac{M-\sqrt{1+p^2}}{1-M^2} - \mathrm{i}p\frac{y}{\sqrt{1-M^2}}\right]}}{4\pi\sqrt{(1-M^2)(1+p^2)}} dp$$

We then have to find a path in the complex plane so that

$$(x+h)\frac{M-\sqrt{1+p^2}}{1-M^2} - \mathrm{i}p\frac{y}{\sqrt{1-M^2}} = -t. \quad (12)$$

We now introduce (r, θ) the "generalized polar coordinates" of (x, y) defined by

$$r^2 = \frac{(x+h)^2}{(1-M^2)^2} + \frac{y^2}{1-M^2}$$

and

$$\cos\theta = \frac{x+h}{r(1-M^2)} \quad \sin\theta = \frac{y^2}{r\sqrt{1-M^2}}.$$

These coordinates are actually "elliptical coordinates": the level lines $r = \text{cst}$ are elipse whereas the level lines $\theta = \text{cst}$ are half-lines.

For $t > t_0 = r(1 - M\cos\theta)$ the solution $p = \gamma^{\pm}(t)$ of (12) are:

$$\gamma^{\pm}(t) = -\mathrm{i}\left(\frac{t}{r} + M\cos\theta \pm \cos\theta\sqrt{\left(\frac{t}{r} + M\cos\theta\right)^2 - 1}\right).$$

As for the acoustic case ($M = 0$) we can now define the path Γ by

$$\begin{cases} \Gamma = \Gamma^+ \cup \Gamma^- \\ \Gamma^{\pm} = \{p = \gamma^{\pm}(t), t_0 \le t\}, \end{cases}$$

and prove that

$$\tilde{G}(x,y,s) = -\int_{\Gamma} \frac{e^{\Sigma(x)\frac{M-\sqrt{1+p^2}}{1-M^2}} e^{s\left[(x+h)\frac{M-\sqrt{1+p^2}}{1-M^2} - \mathrm{i}\,p\frac{y}{\sqrt{1-M^2}}\right]}}{4\pi\sqrt{(1-M^2)(1+p^2)}} dp.$$

After some calculations, we obtain:

- $$\frac{1}{\left(1+\gamma^{\pm 2}(t)\right)^{\frac{1}{2}}}\frac{d\gamma^{\pm}(t)}{dt} = \pm\frac{dt}{\sqrt{(t+Mr\cos\theta)^2 - r^2}}$$
- $$\Sigma(x)\frac{M - \left(1+\gamma^{\pm 2}(t)\right)^{\frac{1}{2}}}{1-M^2} = -A(x,y,t) \mp \mathrm{i}\,B(x,y,t)$$

  with
  - $A(x,y,t) = \Sigma(x)\left(\frac{t}{r}\cos\theta - M\sin^2\theta\right)$;
  - $B(x,y,t) = \Sigma(x)\sin\theta\sqrt{\left(\frac{t}{r} + M\cos\theta\right)^2 - 1}.$

Finally

$$\tilde{G}(x,y,s) = \int_{t_0}^{+\infty} \frac{e^{-A(x,t)}\cos B(x,t)}{2\pi\sqrt{1-M^2}\sqrt{(t+Mr\cos\theta)^2 - r^2}} dt$$

and, by the injectivity of the Laplace transform:

$$G(x,y,t) = \frac{H\left(t - r(1-M\cos\theta)e^{-A(x,t)}\cos\left[B(x,t)\right]\right)}{2\pi\sqrt{1-M^2}\sqrt{(t+Mr\cos\theta)^2 - r^2}}.$$

3.3 Analysis of the instabilities

The instabilities in the PML are obviously produced by the term $\phi(x,y,t) = e^{-A(x,y,t)}$. Since the function $A(x,t)$ is increasing for $t \ge t_0$ its minimum is $A(x,y,t_0) = \Sigma(x)(\cos\theta - M)$ and

$$\max|\phi(x,y,t)|_{t\ge t_0} = e^{-\Sigma(x)(\cos\theta - M)}.$$

Thus, for a given point (x,y), the function $t \to \phi(x,t)$ is bounded. However, if we consider, for a given direction θ_0 and a given time t, the point of generalized coordinates $(r(t),\theta_0)$ where

$$r(t) = \frac{t}{1 - M\cos\theta_0},$$

then

$$\phi(r(t),\theta_0,t) = e^{-\Sigma(x(t))(\cos\theta_0 - M)}.$$

Since x increases when r increases (see Fig. 11), the function $t \to \phi(r(t),\theta_0,t)$ increases exponentially if $\cos\theta_0 < M$. Therefore, though the norm of the solution is bounded at every point with respect to the time, the uniform norm of the solution is exponentially increasing with the time.

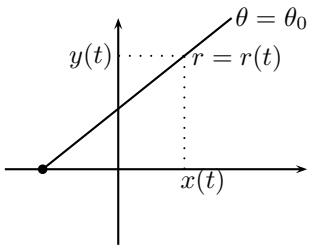

Fig. 11. Position of the point $(r(t),\theta_0)$.

3.4 Numerical results

To illustrate the instabilities in the PML, we have represented the solution u for $M = 0.5$ at different times. The red lines represent the unstable region $\cos\theta_0 < M$, the instabilities are clearly moving with the wave front.

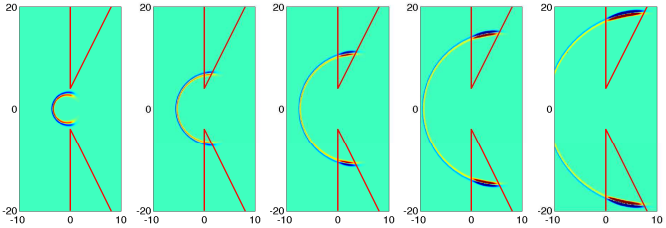

Fig. 12. Instabilities in the PML ($M = 0.5$)

REFERENCES

P. van der Berg A. T. de Hoop and F. Remis. Analytic time-domain performance analysis of absorbing boundary conditions and perfectly matched layers. In *Proc. IEEE Antennas and Propagation Society International Symposium*, volume 4, pages 502–505, 2001.

E. Bécache, S. Fauqueux, and P. Joly. Stability of perfectly matched layers, group velocities and anisotropic waves. *J. Comput. Phys.*, 188(2):399–433, 2003. ISSN 0021-9991.

J.-P. Bérenger. Three-dimensional perfectly matched layer for the absorption of electromagnetic waves. *J. Comput. Phys.*, 127(2):363–379, 1996. ISSN 0021-9991.

L. Cagniard. *Reflexion et refraction des ondes sismiques progressives*. Gauthier-Villard, 1939.

L. Cagniard. *Reflection and refraction of progressive seismic waves*. McGraw-Hill, 1962. Translated from Cagniard (1939).

A. T. de Hoop. The surface line source problem. *Appl. Sci. Res. B*, 8:349–356, 1959.

J. Diaz and P. Joly. An analysis of higher order boundary conditions for the wave equation. *SIAM Journal on Applied Mathematics*, 65(5):1547–1575, 2005.

J. Diaz and P. Joly. A time domain analysis of pml models in acoustics. *Comput. Methods Appl. Mech. Engrg.*, 195 (29-32):3820–3853, 2006.